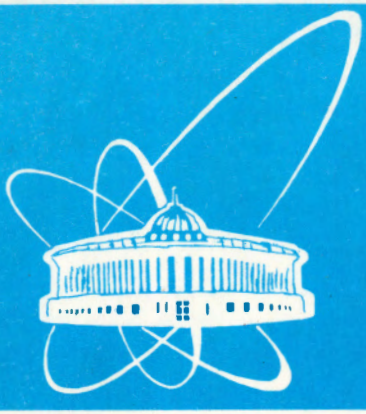

сообщения
объединенного
института
ядерных
исследований
дубна

E11-94-140

P.G.Akishin, I.V.Puzynin, V.V.Starkov, S.I.Vinitsky

ON THE NUMERICAL METHOD FOR ANALYSIS OF THE DYNAMICS OF THE CLASSICAL HAMILTONIAN SYSTEMS

1994

1.INTRODUCTION

In the present paper the numerical analysis method for the dynamics of the classical Hamiltonian systems with pair potentials is described. The Hamiltonian H of such a system of N particles has the form

$$H = \sum_{i=1}^{N} \frac{\vec{p}_i^2}{2m_i} + \sum_{i<j} V_{i,j}(\vec{q}_i - \vec{q}_j) \equiv T + U. \tag{1}$$

The need for the analysis of such systems often arises in investigations of models in theoretical and experimental physics [1-5]. The problem is reduced to the solution of the nonlinear equations of motion

$$\frac{d\vec{q}_i}{dt} = \frac{\partial H}{\partial \vec{p}_i}, \qquad \frac{d\vec{p}_i}{dt} = -\frac{\partial H}{\partial \vec{q}_i}, \tag{2}$$

with the given initial conditions

$$\vec{q}_i(t_0) = \vec{q}_i^{\,0}, \qquad \vec{p}_i(t_0) = \vec{p}_i^{\,0}, \tag{3}$$

the independent variable t varying within a sufficiently large interval, $0 \le t \le T$, $T \gg 1$. Moreover, in a number of physical cases of interest it is necessary to know with the given accuracy the asymptotic behavior of the solutions when $T \to \infty$.

Only in extremely rare cases it appears to be possible to find the analytical solution of the Cauchy problem (2), (3). Therefore, the numerical methods are the main tool for solving this problem. General methods of the Runge-Kutta type [6] and corresponding programs, developed for a wide variety of equations, are often used in this case without taking the specific features of the problem (2), (3) into account. This results in the unjustifiable complication of the computations and sometimes even in the loss of the accuracy [7,8].

In contrary to such an approach, we develop our numerical algorithm basing on the Taylor decomposition of the solution to be found, supposing that the terms of this series may be expressed analytically. This supposition is justified for some potentials V_{ij} important in physics. This allows us to choose efficiently the integration step depending on the behavior of the series truncation error, and also to carry out the parallel analysis of the small perturbation dynamics, which, in turn, makes it possible to reason about such properties of the system as the stability and the transition to chaotic regime [9] .

In Section 2 the proposed method and algorithm are described. In Section 3 the results of the calculations and the numerical analysis of the system dynamics are presented for some classical potentials - Coulomb, Gaussian, Toda and Henon-Heiles [2]. The analysis carried out shows that in some cases the so-called unstable regime is a computational effect.

2.NUMERICAL INTEGRATION METHOD

To get an approximate solution of the Cauchy problem (2), (3) in this paper the Taylor expansion of the solution in the vicinity of the point t is used.

Suppose that at a certain moment t of time the radius-vectors $\{\vec{q}_i(t)\}$ and the momenta $\{\vec{p}_i(t)\}$ are known. Taking a derivative of Eq. (2) with respect to t yields

$$\frac{d^2\vec{q}_i(t)}{dt^2} = \frac{d}{dt}\left(\frac{\partial H(t)}{\partial \vec{p}_i}\right) = \sum_{j=1}^{N}\left[\frac{\partial^2 H}{\partial \vec{p}_i \partial \vec{p}_j}\frac{d\vec{p}_j}{dt} + \frac{\partial^2 H}{\partial \vec{p}_i \partial \vec{q}_j}\frac{d\vec{q}_j}{dt}\right]. \tag{4}$$

Making use of Eq. (2), one gets

$$\frac{d^2\vec{q}_i(t)}{dt^2} = \sum_{j=1}^{N}\left[-\frac{\partial^2 H}{\partial \vec{p}_i \partial \vec{p}_j}\frac{\partial H}{\partial \vec{q}_j} + \frac{\partial^2 H}{\partial \vec{p}_i \partial \vec{q}_j}\frac{\partial H}{\partial \vec{p}_j}\right], \quad i = 1, \ldots, N. \tag{5}$$

In a similar way the following expression for the second derivatives may be obtained

$$\frac{d^2\vec{p}_i(t)}{dt^2} = \sum_{j=1}^{N}\left[\frac{\partial^2 H}{\partial \vec{q}_i \partial \vec{p}_j}\frac{\partial H}{\partial \vec{q}_j} - \frac{\partial^2 H}{\partial \vec{q}_i \partial \vec{q}_j}\frac{\partial H}{\partial \vec{p}_j}\right], \quad i = 1, \ldots, N. \tag{6}$$

Supposing that for the Hamiltonian considered it is possible to get analytical expressions for the partial derivatives in all variables up to the order of $n+1$ and using the similar recursion procedure one can find n derivatives of $\{\vec{q}_i(t)\}$ and $\{\vec{p}_i(t)\}$ with respect to t.

Note that for any vector function $\vec{r}(t)$, differentiable $n+1$ times in the interval $[t, t+\Delta t]$, the following identity is valid

$$\vec{r}(t+\Delta t) - \sum_{j=0}^{n}\frac{\vec{r}^{(j)}(t)(\Delta t)^j}{j!} = \frac{\vec{r}^{(n+1)}(\xi)(\Delta t)^{n+1}}{(n+1)!}, \tag{7}$$

where $\vec{r}^{(j)}(t)$ is the j-th derivative of $\vec{r}(t)$ at the point t, and ξ belongs to the interval $[t, t+\Delta t]$. Replacing the right-hand side of equation (7) with zero we get an approximate equation for $\vec{r}(t+\Delta t)$. Varying the integration step Δt, one can control the error, contributed to Eq. (7). Supposing that the variation of $\vec{r}^{(n+1)}(\xi)$ is small within the interval $[t, t+\Delta t]$ and setting the accuracy ϵ for the local error, it is possible to express the integration step in time as

$$\Delta t = \sqrt[n+1]{\frac{\epsilon(n+1)!}{|\vec{r}^{(n+1)}(t)|}}. \tag{8}$$

Let us consider $\vec{r}(t) = (\vec{q}_1(t), \ldots, \vec{q}_N(t), \vec{p}_1(t), \ldots, \vec{p}_N(t))^T$ as the vector function $\vec{r}(t)$ and make use of Eqs. (7) and (8). Then the values $\{\vec{q}_i\}$ and $\{\vec{p}_i\}$ at the point $t+\Delta t$ may be found.

The additional control of accuracy may be realized by means of checking the conservation laws for the energy E and the momentum $\vec{P}$, which are valid for the system (2), (3) with the Hamiltonian (1):

$$H(t) = H(t_0) = E = \text{const}, \qquad \vec{P}(t) = \sum_{i=1}^{N} \vec{p}_i(t) = \sum_{i=1}^{N} \vec{p}_i(t_0) = \vec{P}^0. \tag{9}$$

Within the framework of the approach considered the proposed algorithm may be also applied to the analysis of the dynamics of small deviations $\{\Delta\vec{q}_i\}$ and $\{\Delta\vec{p}_i\}$ of the coordinates $\{\vec{q}_i\}$ and momenta $\{\vec{p}_i\}$. The linearized set of equations (2), describing the propagation dynamics for small perturbations of the solution in time, has the form

$$\frac{d\Delta\vec{q}_i}{dt} = \sum_{j=1}^{N} \left[\frac{\partial^2 H}{\partial\vec{p}_i \partial\vec{q}_j} \Delta\vec{q}_j + \frac{\partial^2 H}{\partial\vec{p}_i \partial\vec{p}_j} \Delta\vec{p}_j \right],$$

$$\frac{d\Delta\vec{p}_i}{dt} = \sum_{j=1}^{N} \left[-\frac{\partial^2 H}{\partial\vec{q}_i \partial\vec{q}_j} \Delta\vec{q}_j - \frac{\partial^2 H}{\partial\vec{q}_i \partial\vec{p}_j} \Delta\vec{p}_j \right]. \tag{10}$$

Let us write this set in the matrix form

$$\frac{d\vec{z}}{dt} = \begin{pmatrix} \hat{0} & \hat{I} \\ -\hat{S}(t) & \hat{0} \end{pmatrix} \vec{z} \equiv \hat{B}(t)\vec{z}, \qquad \vec{z}(t_0) = \vec{z}^0, \tag{11}$$

where $\vec{z} = (\Delta\vec{q}_1, \ldots, \Delta\vec{q}_N, \Delta\vec{p}_1, \ldots, \Delta\vec{p}_N)^T$ is the complete set of small deviations, $\hat{0}$ and $\hat{I}$ are the zero and unity matrices, respectively. The matrix $\hat{S}(t)$ in (11) is a symmetrical block-structure matrix composed of blocks

$$\left\{ \hat{S}_{ij}(t) \right\}_{i,j=1}^{N}$$

of the second derivatives of the total potential energy $U \equiv U(\vec{q}_1, \ldots, \vec{q}_N)$ along the trajectory of motion $\vec{q}_i \equiv \vec{q}_i(t)$:

$$\hat{S}_{ij}(t) = \frac{\partial^2 U(\vec{q}_1, \ldots, \vec{q}_N)}{\partial\vec{q}_i \partial\vec{q}_j}. \tag{12}$$

It is known that the local stability of the solutions of the problem (2), (3) may be controlled by means of the analysis of the spectrum of the matrix $\hat{B}(t)$ entering Eq. (11). If the real part of the spectrum $\sigma(\hat{B})$ of the matrix $\hat{B}(t)$ is strictly negative, the asymptotic stability of the solution with respect to small deviations takes place. If the real part of the spectrum is positive, $\mathrm{Re}(\sigma(\hat{B})) > 0$, small deviations increase exponentially in the vicinity of the point t.

Being realized as the program BODYN, the algorithm described above allows one to analyse both the dynamics of the trajectories in the phase space and their local stability at a fixed point of the phase space. The program is written in FORTRAN-77 and installed on the EC-1066 (IBM) type of computer. In this particular program the fourth order of the Taylor expansion in the time step Δt is used.

3.NUMERICAL STUDY OF SOME HAMILTONIAN SYSTEMS

In the present section we describe the peculiarities of the numerical analysis of the dynamics of some Hamiltonian systems by means of the algorithm presented above.

A. Toda and Henon-Heiles models

Consider the Hamiltonian (1) for a system of three "one-dimensional" particles ($N = 3$), corresponding to the Toda and Henon-Heiles models [2]

$$H = \frac{1}{2}(p_1^2 + p_2^2 + p_3^2) + U(q_1, q_2, q_3), \tag{13}$$

where

$$U(q_1, q_2, q_3) = V(q_1 - q_2) + V(q_2 - q_3) + V(q_3 - q_1) - 3$$

is the potential energy of the system. Here

$$V(q) = \exp(q) \tag{14}$$

is the pair interaction potential for the Toda model and

$$V(q) = 1 + \frac{1}{2}q^2 + \frac{1}{3}q^3 \tag{15}$$

is the pair interaction potential for the Henon-Heiles model.

The generalization of the Henon-Heiles model is described by the following pair interaction potential

$$V(q) = 1 + \sum_{i=2}^{M} \frac{q^i}{i!}. \tag{15a}$$

For these models the energy and momentum conservation laws hold

$$H(t) = H(t_0) = E = \text{const}$$

$$P(t) = p_1(t) + p_2(t) + p_3(t) = P(t_0) = P = \text{const}. \tag{16}$$

Note that in the present algorithm the momentum conservation law is valid automatically for pair potentials. Since the Toda model is a completely integrable system, the third, additional, time-independent integral of motion exists for it, namely

$$I(t) = p_1(t)p_2(t)p_3(t) - p_1(t)s_2(t) - p_2(t)s_3(t) - p_3(t)s_1(t) = I(t_0) = I = \text{const}, \tag{17}$$

where

$$s_1(t) = \exp(q_1(t) - q_2(t)), \qquad s_2(t) = \exp(q_2(t) - q_3(t)),$$
$$s_3(t) = \exp(q_3(t) - q_1(t)), \tag{17'}$$

are the pair interaction potentials.

It is known that for some initial data Hamiltonian systems like Henon-Heiles model pass through unstable and chaotic regimes. One of the mechanisms responsible for these regimes in deterministic systems is the local instability which causes the exponential divergence of initially close trajectories in the phase space [9].

Consider for the models studied a set of linearized equations (11) for the small deviations $\vec{z}(t)$ for $N = 3$. Remind that the local behaviour of $\vec{z}(t)$ in the vicinity of each t value is determined by the spectrum of the matrix $\hat{B} = \hat{B}(t)$. This spectrum may be expressed via the spectrum of the matrix $\hat{S} = \hat{S}(t)$. The matrix $\hat{S}$ is symmetrical, hence its spectrum $\sigma(\hat{S}) = \{\lambda_i\}_{i=1}^3$ is real. Respectively, the spectrum of the matrix $\hat{B}$ is $\sigma(\hat{B}) = \{\pm\sqrt{-\lambda_i}\}_{i=1}^3$. Then the solution $\vec{z}(t)$ in the vicinity of t may be presented as

$$\vec{z}(t) = \sum_{i=1}^{3} \left(e^{-\sqrt{-\lambda_i}t}\vec{u}_i + e^{+\sqrt{-\lambda_i}t}\vec{v}_i \right). \tag{18}$$

It follows from (18) that if at least one of $\{\lambda_i\}_{i=1}^3$ is negative, we have the exponential growth of the small deviation $\vec{z}(t)$. For the Toda model the matrix $\hat{S}$ looks as

$$\hat{S} = \begin{pmatrix} s_1 + s_3 & -s_1 & -s_3 \\ -s_1 & s_1 + s_2 & -s_2 \\ -s_3 & -s_2 & s_2 + s_3 \end{pmatrix}. \tag{19}$$

where s_1, s_2, s_3 are defined in (17). The eigenvalues of the symmetrical matrix $\hat{S}$ are

$$\lambda_1 = 0, \qquad \lambda_{2,3} = V_0 \pm \sqrt{V_0^2 - 3V_0}, \tag{20}$$

where $V_0 = s_1 + s_2 + s_3$, $\quad V_0 > 0$. It follows that all the eigenvalues λ_i for the Toda model are always non-negative for any initial data. Therefore, the chaotic regime does not occur, since the exponents in (18) are either purely imaginary, or zero.

A different situation may occure for the Henon-Heiles model. The eigenvalues λ_i of the matrix $\hat{S}$ may appear to be negative, i.e., the chaotic regime arises since the exponents in (18) become positive. The explicit expression of the eigenvalues λ_i has the form

$$\lambda_1 = 0, \qquad \lambda_{2,3} = (G_1 + G_2 + G_3) \pm \sqrt{(G_1 + G_2 + G_3)^2 - 3(G_1G_2 + G_2G_3 + G_3G_1)}, \tag{21}$$

where

$$G_1 = 1 + 2(q_2 - q_1), \qquad G_2 = 1 + 2(q_3 - q_2), \qquad G_3 = 1 + 2(q_1 - q_3).$$

If the values of q_i are such that $(G_1G_2 + G_2G_3 + G_3G_1) < 0$, then one of the values λ_i is negative and the small deviations demonstrate the exponential growth. Therefore, as a result of the long presence of the trajectory in this region, the motion becomes chaotic.

Using the algorithm proposed the particle trajectories have been calculated for the Toda model. The validity of the conservation laws for the energy (16) and the additional integral $I(t)$ (17), depending on the prescribed upper limit of the local error ϵ and the time t, is shown in Tables 1 and 2 , respectively. In the same tables the mean step value $\Delta t_{av} = (t - t_0)/k$, where (t_0, t) is the integration interval in time, k is the number of the integration steps, is presented as one of the characteristics of the algorithm. In Table 3 the dependence of the coordinates $q_i(t)$ and momenta $p_i(t)$

upon the value of ϵ is shown. This Table demonstrates the influence of the summary error upon the results in all the integration interval (t_0, t). Analogous results in case of the stable regime were obtained for the Henon-Heiles model. They are illustrated in Tables 4–6.

The results of calculations of unstable computational regime are shown in Tables 7–9 for the Henon-Heiles model . It may be seen from Table 9 that in case of unstable computational regime the coordinates $q_i(t)$ and the momenta $p_i(t)$ cannot be determined with the prescribed accuracy. In Tables 10, 11 the dependence of minimal eigenvalues $\{\lambda_3\}$ of the matrix $\hat{S}$ upon t and ϵ is demonstrated for the Henon-Heiles model in stable and unstable computational regimes. For comparison in Table 12 the same dependence is shown for the Toda model.

Another mechanism responsible for the unstable calculational regime is the local unstability which causes large deviations between positive eigenvalues $\{\lambda_i\}$. In Table 13 the dependence of deviations between eigenvalues $\{\lambda_3\}$ and $\{\lambda_1\}$ of the matrix $\hat{S}$ upon t and M is demonstrated for the generalized Henon-Heiles model. For odd and even numbers of potential we have unstable and stable regimes correspondingly. Unstability of calculations in the considered example is result of large magnitudes of egenvalues $\{\lambda_2\}$and $\{\lambda_3\}$ of the matrix $\hat{S}$ upon t ($\lambda_1 = 0$). In this case the supposition about small variation of $\vec{r}^{(n+1)}(\xi)$ within the interval $[t, t + \Delta t]$ is not valid for proposed method. It should be noted that the same situation holds in another approach like Runge-Kutta type methods. As it follows from our analysis the result obtained in unstable regime is rather a consequence of the computational effects (error accumulation, the limited number of digits, etc.) than a reflection of the real picture. The latter should be obtained by means of the specially designed algorithms, analogous to those applied to the solution of the hard differential equation sets [6].

B. System of similar particles with Coulomb and Gaussian potentials

Test calculations for similar charged Coulomb particles having the unit masses and charges have been also carried out to check up the accuracy of the method. At the initial moment $t_0 = 0$ of time all the particles were considered to be placed in the apexes of the rectilinear octagon inscribed in a unit circle, the velocities of the particles being equal in absolute values and directed along the radius-vectors $\{\vec{q}_i\}$ towards the center. It follows from the symmetry of the problem that at any moment t of time each of the particles will move along the ray passing from the center via the initial position of the particle. The results of checking up the validity of the conservation laws are presented in Table 14. From this Table one can also see the dependence of the energy $E(t)$, coordinate $q_1(t)$, momentum $p_1(t)$ and the mean step value δt_{av} upon the value of the local error ε and stability of calculations up to the time as large as $t = 1000$. The mean time of one calculation was from 0.1 to 4 s using the EC-1060 computer.

This configuration of material points has also been calculated for the potentials V_{ij} having the Gaussian form

$$V_{ij}(\vec{q}_i - \vec{q}_j) = \alpha \exp\{-\beta|\vec{q}_i - \vec{q}_j|^2\}.$$

The corresponding results for $\alpha = 1.$, $\beta = 0.1$ are shown in Table 15.

So, the calculation technique developed may be extended over the class of potentials, for which it appears to be possible to write explicitly the partial derivatives of the Hamiltonian with respect to the phase variables.

It should be noted that the program realizing the method proposed is included into the system for modelling the events in the experimental setup "FOBOS" in the Laboratory of Nuclear Reactions, JINR.

4.CONCLUSION

The algorithm proposed for the class of problems considered seems to be more efficient compared to general methods of the Runge-Kutta type. This is confirmed by the successful operation of the corresponding program included into the modelling system of the experimental setup, where the mass calculations are realized. As compared with the standard programs, the program based on this algorithm has the advantage of the possibility to analyze the stability of the solutions, which permits one to evaluate the reliability of the results. The latter is particularly important in the studies of chaotic regimes in Hamiltonian systems and, in principle, makes it possible to judge whether the chaotic regime is really the essence of the phenomena considered or it is a computational effect.

The prospects of developing the algorithms, combining the calculations of the system dynamics with the stability analysis, are promising in modelling the complex behaviour of simple systems.

Acknowledgements

We are indebted to Profs. I. Antoniou, N. Chekanov and V. Derbov for fruitful discussion. We thank the Commission of the European Communities for partial financial support in the frame of EC-Russia collaboration Contract No.ECRU002.

Table 1:

The dependence of the energy $E(t)$, the additional integral of motion $I(t)$ and the mean step value $\delta t_{av} = (t - t_0)/k$ (where (t_0, t) is the integration interval in time, k is the number of the integration steps) upon the value of the local error ε (see eq.(8)) in the Toda model for the value of time $t = 20$

ε	$E(t)$	$I(t)$	δt_{av}
10^{-4}	21.0702	-1.24645	0.05958
10^{-6}	21.5681	-0.89949	0.01888
10^{-8}	21.5883	-0.88543	0.00598
10^{-10}	21.5889	-0.88494	0.00189

Table 2:

The lependence of the energy $E(t)$ and the additional integral of motion $I(t)$ upon the value of time t for the value of the local error $\epsilon = 10^{-6}$ in the Toda model

t	$E(t)$	$I(t)$
0.	21.5889	-0.88492
4.	21.5856	-0.88867
8.	21.5820	-0.89008
12.	21.5739	-0.89325
16.	21.5702	-0.89552
20.	21.5681	-0.89948

Table 3:

The dependence of the coordinates $q_i(t)$ and momenta $p_i(t)$ upon the value of the local error ϵ in the Toda model for the value of time $t = 20$

ϵ	$q_1(t)$	$q_2(t)$	$q_3(t)$	$p_1(t)$	$p_2(t)$	$p_3(t)$
10^{-4}	11.992	15.396	14.010	3.9803	-1.7722	-0.1881
10^{-6}	12.190	15.259	13.949	4.4653	-1.9611	-0.4842
10^{-8}	12.199	15.253	13.946	4.4835	-1.9680	-0.4954
10^{-10}	12.200	15.253	13.946	4.4840	-1.9682	-0.4958

Table 4:

The dependence of the energy $E(t)$ and the mean step value $\delta t_{av} = (t - t_0)/k$ upon the value of the local error ϵ in the case of stable regime of the Henon-Heiles model for the value of time $t = 2.5$

ϵ	$E(t)$	δt_{av}
10^{-2}	7.103314	0.13853
10^{-4}	7.100485	0.03510
10^{-6}	7.100033	0.00788
10^{-8}	7.100000	0.00171

Table 5:

The dependence of the energy $E(t)$ upon the value of time t and the value of the local error ϵ in the case of stable regime of the Henon-Heiles model

	$t = 0.$	$t = 0.5$	$t = 1.$	$t = 1.5$	$t = 2.$
$\epsilon = 10^{-2}$	7.1000	7.0613	7.0613	7.0903	7.0982
$\epsilon = 10^{-4}$	7.1000	7.0987	7.0960	7.0986	7.0996
$\epsilon = 10^{-6}$	7.1000	7.0999	7.0998	7.0999	7.0999
$\epsilon = 10^{-8}$	7.1000	7.0999	7.0999	7.0999	7.1000

Table 6:

The dependence of the coordinates $q_i(t)$ and momenta $p_i(t)$ upon the value of the local error ϵ in case of stable regime of the Henon-Heiles model for the value of time $t = 2$

ϵ	$q_1(t)$	$q_2(t)$	$q_3(t)$	$p_1(t)$	$p_2(t)$	$p_3(t)$
10^{-2}	0.7894	3.2704	2.0581	0.7273	1.5971	-1.8772
10^{-4}	0.6977	3.3885	2.0316	0.5136	1.8126	-1.8790
10^{-6}	0.6930	3.3946	2.0303	0.5020	1.8241	-1.8789
10^{-8}	0.6928	3.3949	2.0302	0.5014	1.8246	-1.8789

Table 7:

The dependence of the energy $E(t)$ and the mean step value $\delta t_{av} = (t - t_0)/k$ upon the value of the local error ϵ in the case of chaotic regime of the Henon-Heiles model for the value of time $t = 4$

ϵ	$E(t)$	δt_{av}
10^{-6}	6.898651	0.0011072
10^{-8}	7.090661	0.0008849
10^{-10}	7.099567	0.0001907
10^{-12}	7.099980	0.0000410

Table 8:

The dependence of the energy $E(t)$ upon the value of time t and the value of the local error ϵ in the case of chaotic regime of the Henon-Heiles model

	$t = 0.$	$t = 1.$	$t = 2.$	$t = 3.$
$\epsilon = 10^{-6}$	7.10000	7.09982	7.09998	7.10005
$\epsilon = 10^{-8}$	7.10000	7.09999	7.09999	7.10000
$\epsilon = 10^{-10}$	7.10000	7.10000	7.10000	7.10000

Table 9:

The dependence of the coordinates $q_i(t)$ and momenta $p_i(t)$ upon the value of the local error ϵ in case of chaotic regime of the Henon-Heiles model for the value of time $t = 4$

ϵ	$q_1(t)$	$q_2(t)$	$q_3(t)$	$p_1(t)$	$p_2(t)$	$p_3(t)$
10^{-6}	-31.9552	36.7735	1.97060	-278.981	278.188	1.24009
10^{-8}	-32.0793	36.8971	1.97106	-280.523	279.709	1.26143
10^{-10}	-32.0852	36.9029	1.97108	-280.595	279.780	1.26245
10^{-12}	-32.0855	36.9030	1.97109	-280.599	279.783	1.26250

Table 10.

The dependence of the minimal eigenvalue $\{\lambda_3\}$ of the matrix $\hat{S}$ (see eq.(21)) upon t and ϵ for the Henon-Heiles model

	$t = 0.$	$t = 0.5$	$t = 1.$	$t = 1.5$	$t = 2.$	$t = 2.5$
$\epsilon = 10^{-2}$	-3.9282	-1.6777	-1.1034	-1.7202	-4.2363	-4.4438
$\epsilon = 10^{-4}$	-3.9282	-1.6701	-1.1251	-1.8539	-4.4265	-5.0724
$\epsilon = 10^{-6}$	-3.9282	-1.6699	-1.1257	-1.8601	-4.4361	-5.1049
$\epsilon = 10^{-8}$	-3.9282	-1.6699	-1.1257	-1.8601	-4.4366	-5.1065

Table 11:

The dependence of the minimal eigenvalue $\{\lambda_3\}$ of the matrix $\hat{S}$ (see eq.(21)) upon t and ϵ for the Henon-Heiles model

	$t = 0.$	$t = 1.$	$t = 2.$	$t = 3.$	$t = 4.$
$\epsilon = 10^{-6}$	-3.9282	-11.2574	-4.4632	-8.9556	-203.191
$\epsilon = 10^{-8}$	-3.9282	-11.2577	-4.4366	-8.9603	-203.935
$\epsilon = 10^{-10}$	-3.9282	-11.2577	-4.4366	-8.9606	-203.970
$\epsilon = 10^{-12}$	-3.9282	-11.2577	-4.4366	-8.9606	-203.971

Table 12:

The dependence of the minimal eigenvalue $\{\lambda_3\}$ of the matrix $\hat{S}$ (see eq.(20)) upon t and ϵ for the Toda model

	$t = 0.$	$t = 4.$	$t = 8.$	$t = 12.$	$t = 16.$	$t = 20.$
$\epsilon = 10^{-4}$	0.75379	2.41311	8.66217	2.43797	1.62631	5.06550
$\epsilon = 10^{-6}$	0.75379	2.40225	8.60587	2.64877	1.72674	4.50984
$\epsilon = 10^{-8}$	0.75379	2.40163	8.60291	2.65849	1.73120	4.48662
$\epsilon = 10^{-10}$	0.75379	2.40160	8.60279	2.65883	1.73128	4.48596

Table 13:

The dependence of deviations between eigenvalues $\{\lambda_3\}$ and $\{\lambda_1\}$ of the matrix $\hat{S}$ upon t and M (see eq.(20)) of potential for the generalized the Henon-Heiles model

	$t = 0.2$	$t = 0.4$	$t = 0.6$	$t = 0.8$	$t = 1.$	$t = 1.2$
$M = 3$	1.178	1.865	1.799	5.708	26.327	157.857
$M = 4$	1.354	1.692	3.455	10.314	12.203	2.952
$M = 5$	1.493	1.737	4.896	30.475	2799.2	> 10000.
$M = 6$	1.603	1.867	6.098	17.115	4.633	1.369
$M = 7$	1.666	1.957	7.164	48.395	>10000.	-
$M = 8$	1.700	2.011	7.503	19.857	4.723	1.668
$M = 9$	1.715	2.035	7.818	37.295	>10000.	-
$M = 10$	1.721	2.046	7.856	23.443	7.573	2.643

Table 14:

The dependence of the energy $E(t)$, coordinate $q_1(t)$, momentum $p_1(t)$ and the mean step value δt_{av} upon the value of the local error ε for the system of the eight similar charged Coulomb particles,the unit masses and charges at the moment $t = 1000$ of time *

ε	$E(t)$	$q_1(t)$	$p_1(t)$	δt_{av}
10^{-2}	23.17997	2403.480	2.406794	76.769
10^{-4}	26.41664	2567.007	2.569431	23.039
10^{-6}	26.43974	2568.152	2.570555	6.9891
10^{-8}	26.43897	2568.114	2.570517	2.1881
10^{-10}	26.43893	2568.112	2.570515	0.6892

* At the initial moment $t_0 = 0$ of time all the particles were considered to be placed in the apexes of the rectilinear octagon inscribed in unit circle, the velocities of particles being equal in absolute values and directed along the radius-vectors $\vec{q}_i(t)$ towards the center.

Table 15:

The dependence of the energy $E(t)$, coordinate $q_1(t)$, momentum $p_1(t)$ and the mean step value δt_{av} upon the value of the local error ε for the system of the eight similar particles with pair Gaussian potentials($\alpha = 1, \beta = 0.1$) at the moment $t = 6$ of time *

ε	$E(t)$	$q_1(t)$	$p_1(t)$	δt_{av}
10^{-2}	14.31632	8.71397	1.88565	1.83617
10^{-4}	23.75530	11.2764	2.43673	0.35703
10^{-6}	23.92727	11.3886	2.44557	0.10659
10^{-8}	23.92547	11.3898	2.44547	0.03354

*The configuration of particles at the initial moment of time was the same as in previous example.

REFERENCES

1. G.Nicolis and I.Prigogine. Exploring Complexity. W.H.Freeman and Co., N.Y., 1989.

2. M.Toda. Theory of Nonlinear Lattice. Springer-Verlag, N.Y.. 1981.

3. Yu.L.Bolotin, S.I.Vinitsky, V.Yu.Gonchar, and N.A Chekanov. Yadern. Fiz.,1989, vol. 50, p. 563–570.

4. Yu.L.Bolotin *et.al.*. Stochastic Nuclear Dynamics. Physics of Elementary Particles and Atomic Nuclei, 1989, vol. 20, No.4, p. 878–929 (in Russian)

5. H.G.Ortlepp and K.D.Schilling. FOBOS — a 4π -Fragment Spectrometer for Heavy-Ion Reaction Products, FZR 92–11, Rosserdor, 1992.

6. H.J.Stetter. Analysis of Discretization Methods for Ordinary Differential Equations. Springer-Verlag, N.Y., 1973.

7. L.G.Ixaru. Numerical Methods for Differential Equations and Applications (Mathematics and its Applications: Fast European Series). Editra Academei, Bucharest, Romania; D.Reidel Publishing Co., Dortrecht/Boston/Lancaster, 1984.

8. K.Feng and M.-z Qin. Comput.Phys.Com. 1991, vol.65, No.1-3, 173-187.

9. L.E.Reichl. The Transition to Chaos. Springer-Verlag, New-York, Inc. 1992.

Received by Publishing Department
on April 20, 1994.